7-1-2010

Scaled Vapor-to-Liquid Nucleation in a Lennard-Jones System

Barbara N. Hale
Missouri University of Science and Technology, bhale@mst.edu

Mark Thomason

Recommended Citation
B. N. Hale and M. Thomason, "Scaled Vapor-to-Liquid Nucleation in a Lennard-Jones System," *Physical Review Letters*, vol. 105, no. 4, American Physical Society (APS), Jul 2010.
The definitive version is available at https://doi.org/10.1103/PhysRevLett.105.046101

Scaled Vapor-to-Liquid Nucleation in a Lennard-Jones System

Barbara N. Hale and Mark Thomason

Physics Department, Missouri University of Science & Technology, Rolla, Missouri 65409

(Received 28 February 2010; published 21 July 2010)

Scaling of the homogenous vapor-to-liquid nucleation rate, J, is observed in a model Lennard-Jones (LJ) system. The model uses Monte Carlo simulation–generated small cluster growth to decay rate constant ratios and the kinetic steady-state nucleation rate formalism to determine J at four temperatures below the LJ critical temperature, T_c. When plotted vs the scaled supersaturation, $\ln S/[T_c/T-1]^{3/2}$, the values of $\log J$ are found to collapse onto a single line. A similar scaling has been observed for the experimental nucleation rate data of water and toluene.

DOI: 10.1103/PhysRevLett.105.046101 PACS numbers: 82.60.Nh, 64.60.qe, 64.70.F−

Nucleation, the process by which embryos of the new phase are formed in a first-order phase transition, occurs in many everyday processes including droplet, aerosol and ice formation in the atmosphere, and in a host of industrial processes which break down complex vapors into their constituents or form alloys and crystalline structures from the liquid melt. Early in the 20th century a simple classical nucleation theory (CNT) [1,2] for predicting the rate of vapor-to-liquid nucleation was developed and used with considerable success to predict onset conditions. In its simplest form this model used the bulk liquid surface tension to determine the free energy of formation of the n-atom cluster from the vapor. However, when it became possible in the 1980s to measure nucleation rates as a function of temperature and for a range of supersaturations [3–8], it was found that the data displayed a temperature dependence which was not consistent with CNT. Several modifications to the classical nucleation theory were proposed in the early 1990s [9–11], the most important correcting the failure of the classical model's cluster free energy of formation to reduce to zero for the monomer (see, for example, Ref. [12]). In the last two decades extensive computer simulations have been undertaken to examine the microscopic nature of the small clusters and the nucleation process [13–40]. In many of these efforts, the temperature dependence of the nucleation rate was greatly improved.

In the late 1980s it was noted that the nucleation rate data exhibited a temperature scaling [41]. An example of this scaling phenomenon for toluene [42] is shown in Fig. 1. Figure 1(a) shows the nucleation rates for six temperatures plotted vs $\ln S$. When plotted in Fig. 1(b) vs $\ln S$ divided by $[T_c/T-1]^{3/2}$, the temperature lines collapse onto a single line. The experimental supersaturation ratio, S, is given by the ratio of vapor pressures, $P/P_{\text{coexistence}}$, and T_c is the critical temperature for toluene. The collapse of the temperature lines indicates that J is not a function of independent variables, S and T, but of the scaling function, $\ln S_c \equiv \ln S/[T_c/T-1]^{3/2}$. A similar scaling occurs for homogeneous nucleation rate data of water [43,44]. The scaling function, $\ln S_c$, is similar to the *scaled supersaturation* used by Binder [45] near the critical point. Two features of the present scaling are different, however: the critical exponents are replaced by the volume to surface dimension ratio, $3/2$, and the temperature, T, of the rate data is far below the critical point, in the range of $T = 0.5T_c$.

It was known that the scaling function, $\ln S_c$, appears in the classical model cluster free energy of formation as $[16\pi\Omega^3/3]/[\ln S_c]^2$ if one assumes a surface tension for the small clusters of the form $\sigma_0'[T_c - T]$, where σ_0' is a constant [41]. The Ω is the excess surface entropy per atom in units of k, the Boltzmann constant. However, the monomer flux factor in the classical nucleation rate (CNT) has an exponential temperature dependence of the form $P/P_c \cong \exp[-W_o(T_c/T-1)]$ which destroys the scaling [42,44]. For argon $W_o \simeq 5$. Some time ago it was proposed that this P/P_c temperature dependence is canceled by extra terms in the free energy of formation generated as one sums discretely over the smallest cluster free energy differences [42]. Unfortunately, how this arises in a first-

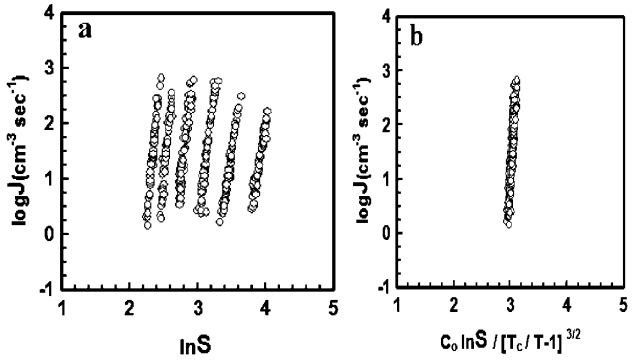

FIG. 1. The homogeneous vapor-to-liquid nucleation rate data of Schmitt *et al.* [4] for toluene at temperatures 265, 255, 245, 235, 225 and 215(±1) K (left to right) plotted vs (a) $\ln S$, and (b) $\ln S/[T_c/T-1]^{3/2}$. The normalization constant, C_o, is $[T_c/235-1]^{3/2}$ and $T_c = 591.8$ K.

principles model of the vapor-to-liquid nucleation has remained largely unexplained.

The goal of the present work has been to generate the nucleation rate in a purely statistical mechanical treatment of small cluster partition functions to see if, indeed, one obtains scaling such as that shown in Fig. 1. In the present study we use the Monte Carlo method to generate growth to decay rate constant ratios for small clusters in a dilute Lennard-Jones (LJ) vapor. These rate constant ratios are then applied to a kinetic nucleation rate formalism [1,46]. The model system is a classical (full potential) Lennard-Jones dilute vapor with volume, V, composed of a non-interacting mixture of ideal gases with each n-atom cluster size constituting an ideal gas of N_n clusters. The separable classical Hamiltonian gives rise to the following law of mass action for ratios of cluster numbers in terms of classical canonical configurational integrals, Q_n: [15,20,34].

$$\frac{N_n}{N_{n-1}N_1} = \frac{Q_n}{Q_{n-1}Q_1 n} = \frac{\beta_{n-1}}{\alpha_n}. \tag{1}$$

At equilibrium in volume, V, detailed balance, $N_n\alpha_n = \beta_{n-1}N_1N_{n-1}$, is maintained. The kinetic nucleation rate formalism (which uses steady-state cluster size numbers, N_n^s) assumes $N_n^s\alpha_n = \beta_{n-1}N_1^sN_{n-1}^s$ with cluster growth and decay taking place *via* monomers with equilibrium rate constants, β_n and α_n. Using $\rho_1 = \frac{N_1}{V}$ at equilibrium and $J_1 = \beta_1[\rho_1 S]^2$, the steady-state nucleation rate, J, is given by

$$\frac{1}{J} = \frac{1}{J_1} + \sum_{n=2}^{M}\left[\beta_n(\rho_1 S)^2\prod_{j=2}^{n}\frac{\beta_{j-1}N_1 S}{\alpha_j}\right]^{-1}, \tag{2}$$

where M is sufficiently large to ensure convergence. In the above expression $S \equiv N_1^s/N_1$ is the monomer supersaturation ratio. The equilibrium monomer flux on the n-cluster, $\beta_n\rho_1$, is approximated using $\beta_n = (\upsilon_{\mathrm{av}}/4)4\pi r_n^2$ with $[n/\rho_{\mathrm{liq}}] = [4/3]\pi r_n^3$, and $\upsilon_{\mathrm{av}} = [8kT/\pi m]^{1/2}$ [2]. The monomer supersaturation can be put into the calculation of J after the equilibrium ($S = 1$) rate constant ratios are calculated. Bennett [47] Metropolis Monte Carlo simulations are used to determine the canonical partition function ratios in the following expressions: [15]

$$-\delta\Delta F_n \equiv \ln\left[\frac{\beta_{n-1}N_1}{\alpha_n}\right] \tag{3}$$

$$= \ln\left[\frac{Q_n\alpha'}{Q_{n-1}Q_1(\upsilon_n/V)}\frac{\rho_1}{\rho_{liq}}\right] \tag{4}$$

$$= -\delta f_n - \ln\frac{\rho_{liq}}{\rho_1}. \tag{5}$$

The Q_n have been normalized with V^n so that $Q_1 = 1$. In these simulations, the assumed cluster definition is n-atoms constrained within a spherical volume, $\upsilon_n = \alpha' n/\rho_{\mathrm{liq}}$ [13]. The quantity $Q_1(\upsilon_n/V)$ is the scaled simulation volume accessible to the monomer. Formally, the expression in Eq. (4) is independent of the constant, α'. However, volumes too large or too small can place physically unrealistic constraints on the cluster definition. A working range is $5 < \alpha' < 8$ and in the present simulations $\alpha' = 7$ was used. Further details are in Refs. [15,20,34].

The law of mass action calls for the Q_n to sample the same configuration space as Q_{n-1} and Q_1. Equation (4) provides a consistent method of scaling the two volumes, υ_n and V, and a means of calculating ρ_1 for the full LJ potential. In the limit of infinite cluster sizes $-\delta f_n$ approaches $\ln\frac{\rho_{\mathrm{liq}}}{\rho_1}$. Using the Dunikov [48] corresponding states procedure one can estimate the full LJ liquid number density, ρ_{liq}, at the low temperatures used here and from the intercept of $-\delta f_n$ at infinite n one can predict a vapor monomer number density, ρ_1. The simulations are carried out at the LJ reduced temperatures, $Tk/\epsilon \equiv T^* = 0.335$, 0.419, 0.503, and 0.700 corresponding roughly to experimental argon temperatures of $T = 40$, 50, 60, and 83.6 K. The Bennett method [47] is well suited for calculating the free energy differences, δf_n, between the two cluster ensembles: one in which all n-atoms interact normally and a second in which the interaction of one of the atoms is turned off. The simulations produce a sequence of rate constant ratios, $\frac{\beta_{j-1}}{\alpha_j}$, for n ranging from 2 to 192. A reduced LJ critical temperature, $T_c^* = 1.313$ and reduced critical density, $\rho_c^* = 0.317$ are used in the analysis [49]. When the ratio T_c/T is used the reduced temperature notation, T^*, is omitted.

In Fig. 2(a) is a plot of the simulation results for $-\delta f_n$ vs $n^{-1/3}$. The intercepts (17.7, 12.9, 9.90 and 5.98) are extrapolated from a least squares fit to data for $n > 20$. In Fig. 2(b) is shown the $\delta\Delta F_n$ divided by $[T_c/T - 1]$ to

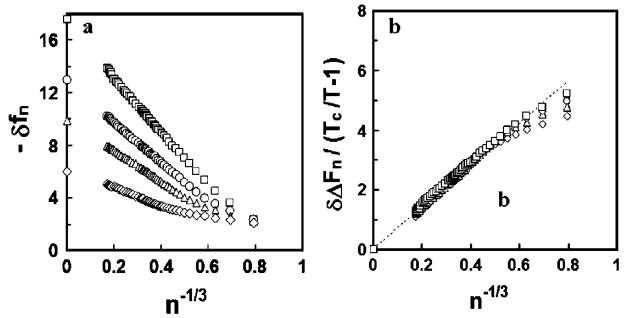

FIG. 2. (a) The $-\delta f_n$ small cluster free energy differences vs $n^{-1/3}$ for the small LJ clusters for $T^* = 0.335$ (□), 0.419 (○), 0.503 (△), and 0.700 (◇) corresponding roughly to argon LJ temperatures of 40, 50, 60, and 83.6 K. The n values range from 2 to 192. The intercepts (17.7, 12.9, 9.90, and 5.98) are extrapolated from a least squares fit to data for $n > 20$. (b) The $\delta\Delta F_n$ for the same n values divided by $[T_c/T - 1]$ where $T_c^* = 1.313$. The dotted line corresponds to a classical LJ model with excess surface entropy/k per atom, $\Omega = 2.19$.

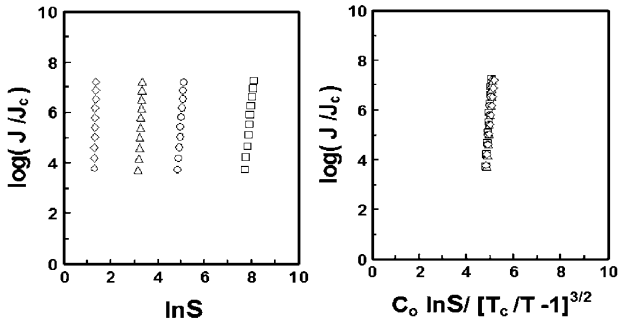

FIG. 3. (a) Nucleation rates, J/J_c, calculated from the Monte Carlo simulation–generated growth to decay rate constant ratios for the model Lennard-Jones system vs ln$S$ at $T^* = 0.335$ (□), 0.419 (○), 0.503 (△), and 0.700 (◇) corresponding roughly to argon LJ temperatures of 40, 50, 60, and 83.6 K. $J_c = \rho_c[40/M]^{1/2}10^{-22}$ s^{-1}. (b) Nucleation rates with the abscissa divided by $[T_c/T - 1]^{3/2}$; $C_o = [T_c^*/0.419 - 1]^{3/2}$.

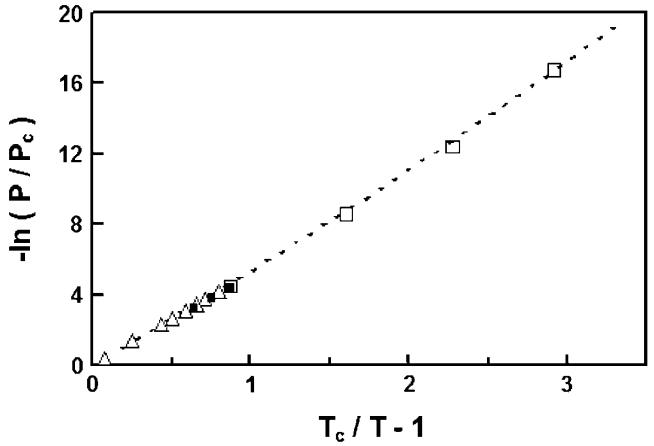

FIG. 4. Corresponding states comparison of $-\ln(P/P_c)$ from the LJ Bennett MC calculations of the present work (□), the argon vapor pressure formula of Fladerer [50] and Iland and Strey [51] (dashed line), the argon experimental vapor pressure data [54] (△), and the LJ Monte Carlo simulations of Chen *et al.* [31] (■).

demonstrate the scaled temperature dependence. An advantage of this analysis is that one can use the scaled quantities to predict nucleation rates at temperatures other than those of the simulation. The slope of the data in Fig. 2(b) is proportional to the effective surface tension of the small clusters [20]. The results are compared with a classical LJ model which corresponds to an excess surface entropy per atom of 2.19 k (the bulk liquid argon value can be estimated from $\sigma_0'/\rho_{\mathrm{liq}}^{2/3} \cong 2.1k$) [41]. Merikanto *et al.* [37,38] have generated similar free energy differences using a modification of the original discrete summation formalism [15] at reduced temperatures of 0.4 and 0.7. However, they do not examine the scaling properties of the free energy differences and their results for $\delta\Delta F_n$ do not scale at small cluster sizes ($n < 20$) because of their cluster definition. Temperatures in the range of 40 K–60 K correspond roughly to those for which argon onset nucleation rates have been measured [50,51].

To demonstrate the scaling of the nucleation rates, values of S are chosen so that the nucleation rates range from 10^4 to 10^7 cm^{-3} s^{-1} for the LJ argon system. To preserve the corresponding states representation, J/J_c is plotted in Fig. 3 where $J_c = \rho_c[40/M]^{1/2}10^{-22}$ s^{-1}, ρ_c is the LJ critical number density and M is the relative atomic mass. Figure 3(a) shows the calculated nucleation rates for the four temperatures plotted vs ln$S$. When plotted in Fig. 3(b) vs the scaled supersaturation, $\ln S/[T_c/T - 1]^{3/2}$, the temperature lines collapse onto a single line. That is, scaling such as that shown in Fig. 1 for the experimental toluene data is observed in the LJ system modeled here. [52,53]

The source of the scaling in the present model is twofold: (1) the corresponding states $[T_c/T - 1]$ temperature dependence of the $\delta\Delta F_n$ [see Fig. 2(b)]; and (2) the discrete summation over the small cluster growth to decay rate constant ratio contributions prescribed by Eq. (2). The latter summation introduces terms (not present in the classical model) which cancel the temperature dependence of the monomer flux factor [42]. One notes that $1/J = \sum_{n=1}^{M}[1/J_n]$, where $J_n = \beta_n\rho_1^2 S^{n+1}\exp[-\sum_{j=2}^{n}\delta\Delta F_j]$.

In obtaining the scaling from the Monte Carlo results, a reliable ρ_1 for the full LJ potential from the intercepts of Fig. 2(a) is essential. Vapor pressures corresponding to these intercepts for the full LJ potential (assuming the vapor consists of monomers only) are shown in Fig. 4. In this figure a Dunikov [48] corresponding states comparison is made with the extrapolated argon vapor pressure formula used by Fladerer [50] and Iland *et al.* [51], experimental data for argon vapor pressure at higher temperatures [54] and the LJ Monte Carlo results of Chen *et al.* [31]. One of the challenges in predicting nucleation rates from potential models is obtaining reliable monomer vapor number densities at low temperatures, where most of the nucleation rate data exist. Equally troublesome for experimentalists can be extrapolating measured vapor pressure data far below the freezing point. A plot such as Fig. 4 can be helpful in evaluating the validity of both approximations.

As far as we are aware, this is the first purely simulation based demonstration of scaling in a model dilute vapor-to-liquid nucleation process. Future applications of this scaling to atmospheric nucleation via molecular-sized heterogeneous sites should be of particular importance [55]. In this case, the scaled supersaturation dependence can survive in the larger growing clusters while the molecularly sized heterogeneity produces an effective reduced excess molecular or atomic entropy at the cluster surface (Ω parameter). This effect is well known in the nucleation of water (and ice) on surfaces, where the contact angle plays the role of a reduced Ω [56]. Applications of the scaling to homogeneous binary vapor-to-liquid nucleation [57] and to ice formation on AgI impurities in supercooled water [58] suggest that this scaling has a wider application. Toward

this end, our hope is that the present simulation results will motivate a more fundamental analysis of scaling in nucleation phenomena, beyond the scope of classical model concepts.

The authors acknowledge G. Wilemski for helpful discussions, J. Kiefer for work done on some of the original LJ cluster simulations and J. Kassner for focusing interest on the scaling approach.

[1] R. Becker and W. Döring, Ann. Phys. (Leipzig) 24, 719 (1935) [online version **416**, 719 (2006)].
[2] M. Volmer and A. Weber, Z. Phys. Chem. **119**, 277 (1926).
[3] R. C. Miller, R. J. Anderson, J. L. Kassner, and D. E. Hagen, J. Chem. Phys. **78**, 3204 (1983).
[4] J. L. Schmitt, R. A. Zalabsky, and G. W. Adams, J. Chem. Phys. **79**, 4496 (1983).
[5] P. E. Wagner and R. Strey, J. Chem. Phys. **80**, 5266 (1984).
[6] G. W. Adams, J. L. Schmitt, and R. A. Zalabsky, J. Chem. Phys. **81**, 5074 (1984).
[7] R. Strey, P. E. Wagner, and T. Schmeling, J. Chem. Phys. **84**, 2325 (1986).
[8] C. Hung, M. J. Krasnopoler, and J. L. Katz, J. Chem. Phys. **90**, 1856 (1989).
[9] G. Wilemski, J. Chem. Phys. **103**, 1119 (1995) gives a comprehensive discussion of the early developments of vapor phase nucleation theory.
[10] D. W. Oxtoby, J. Phys. Condens. Matter **4**, 7627 (1992).
[11] A. Dillmann, Ph.D. thesis, Göttingen, 1989; A. Dillmann and G. E. Meier, J. Chem. Phys. **94**, 3872 (1991).
[12] S. L. Girshick and C. Chiu, J. Chem. Phys. **93**, 1273 (1990).
[13] J. K. Lee, J. A. Barker, and F. F. Abraham, J. Chem. Phys. **58**, 3166 (1973).
[14] N. Garcia and J. M. S. Torroja, Phys. Rev. Lett. **47**, 186 (1981).
[15] B. N. Hale and R. C. Ward, J. Stat. Phys. **28**, 487 (1982).
[16] X. C. Zeng and D. W. Oxtoby, J. Chem. Phys. **95**, 5940 (1991).
[17] X. C. Zeng and D. W. Oxtoby, J. Chem. Phys. **94**, 4472 (1991).
[18] C. Weakliem and H. Reiss, J. Chem. Phys. **99**, 5374 (1993).
[19] D. I. Zhukhovitskii, J. Chem. Phys. **103**, 9401 (1995).
[20] B. Hale, Aust. J. Phys. **49**, 425 (1996).
[21] I. Kusaka, Z. G. Wang, and J. H. Seinfeld, J. Chem. Phys. **108**, 3416 (1998).
[22] K. Yasuoka and M. Matsumoto, J. Chem. Phys. **109**, 8451 (1998).
[23] K. Yasuoka and M. Matsumoto, J. Chem. Phys. **109**, 8463 (1998).
[24] P. R. ten Wolde and D. Frenkel, J. Chem. Phys. **109**, 9901 (1998).
[25] P. R. ten Wolde, M. J. Ruiz-Montero and D. Frenkel, J. Chem. Phys. **110**, 1591 (1999).
[26] K. J. Oh and X. C. Zeng, J. Chem. Phys. **110**, 4471 (1999); *ibid.* **114**, 2681 (2001).
[27] B. Senger, P. Schaaf, D. S. Corti, R. Bowles, D. Pointu, J. C. Voegel, and H. Reiss, J. Chem. Phys. **110**, 6438 (1999).
[28] S. M. Kathmann, G. K. Schenter, and B. C. Garrett, J. Chem. Phys. **111**, 4688 (1999).
[29] S. Wonczak, R. Strey, and D. Stauffer, J. Chem. Phys. **113**, 1976 (2000).
[30] K. J. Oh and X. C. Zeng, J. Chem. Phys. **112**, 294 (2000).
[31] B. Chen, J. I. Siepmann, K. J. Oh, and M. L. Klein, J. Chem. Phys. **115**, 10 903 (2001).
[32] B. N. Hale and S. M. Kathmann, J. Phys. Chem. B **105**, 11 719 (2001).
[33] I. Kusaka, J. Chem. Phys. **119**, 3820 (2003).
[34] B. N. Hale and D. J. DiMattio, J. Phys. Chem. B **108**, 19 780 (2004).
[35] J. Merikanto, E. Zapadinsky, and H. Vehkamäki, J. Chem. Phys. **121**, 914 (2004).
[36] J. Wedekind, J. Wölk, D. Reguera, and R. Strey, J. Chem. Phys. **127**, 154515 (2007).
[37] A. Lauri, J. Merikanto, E. Zapadinsky, and H. Vehkamäki, Atmos. Res. **82**, 489 (2006).
[38] J. Merikanto, E. Zapadinsky, A. Lauri, and H. Vehkamäki, Phys. Rev. Lett. **98**, 145702 (2007).
[39] M. Horsch, J. Vrabec, and H. Hasse, Phys. Rev. E **78**, 011603 (2008).
[40] M. Schrader, P. Virnau, and K. Binder, Phys. Rev. E **79**, 061104 (2009).
[41] B. N. Hale, Phys. Rev. A **33**, 4156 (1986).
[42] B. N. Hale, Metall. Trans. A **23**, 1863 (1992).
[43] J. Wölk and R. Strey, J. Phys. Chem. B **105**, 11683 (2001).
[44] B. N. Hale, J. Chem. Phys. **122**, 204509 (2005).
[45] K. Binder, J. Phys. (Paris), Colloq. **41**, C4-51 (1980); K. Binder and D. Stauffer, Adv. Phys. **25**, 343 (1976).
[46] J. L. Katz and F. Spaepen, Philos. Mag. B **37**, 137 (1978).
[47] C. H. Bennett, J. Comput. Phys. **22**, 245 (1976).
[48] D. O. Dunikov, S. P. Mallyshenko, and V. V. Zhakhovskii, J. Chem. Phys. **115**, 6623 (2001).
[49] J. Perez-Pellitero, P. Ungerer, G. Orkoulas, and A. D. Mackie, J. Chem. Phys. **125**, 054515 (2006).
[50] A. Fladerer and R. Strey, J. Chem. Phys. **124**, 164710 (2006).
[51] K. Iland, J. Wölk, and R. Strey, J. Chem. Phys. **127**, 154506 (2007).
[52] The experimental argon "onset nucleation rates" of Ref. [51] also scale; the S, however, are a factor of 5 smaller than those in Fig. 3 and the excess surface entropy corresponds to $\Omega \cong 1.5$. See Fig. 6 in Ref. [53].
[53] S. Sinha, A. Bhabhe, H. Laksmono, J. Wölk, R. Strey, and B. Wyslouzil, J. Chem. Phys. **132**, 064304 (2010).
[54] R. Gilgen, R. Kleinrahm, and W. Wagner, J. Chem. Thermodyn. **26**, 399 (1994).
[55] P. M. winkler, G. Steiner, A. Vrtala, H. Vehkamäki, M. Noppel, K. E. J. Lehtinen, G. P. Reischl, P. E. Wagner, and M. Kumala, Science **319**, 1374 (2008).
[56] N. H. Fletcher, *The Physics of Rainclouds* (Cambridge, London, 1969), p. 52; , *The Chemical Physics of Ice* (Cambridge, London, 1970), p. 98.
[57] B. N. Hale and G. Wilemski, Chem. Phys. Lett. **305**, 263 (1999).
[58] B. Hale, Lect. Notes Phys. **309**, 321 (1988).